BRAIN
A JOURNAL OF NEUROLOGY

Altered structural connectivity of cortico-striato-pallido-thalamic networks in Gilles de la Tourette syndrome

Yulia Worbe,*,[1,2,3] Linda Marrakchi-Kacem,*,[2,4,5] Sophie Lecomte,[2,4,5] Romain Valabregue,[2,6] Fabrice Poupon,[4] Pamela Guevara,[4] Alan Tucholka,[4] Jean-François Mangin,[4] Marie Vidailhet,[1,2,3] Stephane Lehericy,[2,6] Andreas Hartmann[1,2,3] and Cyril Poupon[4]

*These authors contributed equally to this work.

See Draper and Jackson (doi:10.1093/brain/awu338) for a scientific commentary on this article.

Gilles de la Tourette syndrome is a childhood-onset syndrome characterized by the presence and persistence of motor and vocal tics. A dysfunction of cortico-striato-pallido-thalamo-cortical networks in this syndrome has been supported by convergent data from neuro-pathological, electrophysiological as well as structural and functional neuroimaging studies. Here, we addressed the question of structural integration of cortico-striato-pallido-thalamo-cortical networks in Gilles de la Tourette syndrome. We specifically tested the hypothesis that deviant brain development in Gilles de la Tourette syndrome could affect structural connectivity within the input and output basal ganglia structures and thalamus. To this aim, we acquired data on 49 adult patients and 28 gender and age-matched control subjects on a 3 T magnetic resonance imaging scanner. We used and further implemented streamline probabilistic tractography algorithms that allowed us to quantify the structural integration of cortico-striato-pallido-thalamo-cortical networks. To further investigate the microstructure of white matter in patients with Gilles de la Tourette syndrome, we also evaluated fractional anisotropy and radial diffusivity in these pathways, which are both sensitive to axonal package and to myelin ensheathment. In patients with Gilles de la Tourette syndrome compared to control subjects, we found white matter abnormalities in neuronal pathways connecting the cerebral cortex, the basal ganglia and the thalamus. Specifically, striatum and thalamus had abnormally enhanced structural connectivity with primary motor and sensory cortices, as well as paracentral lobule, supplementary motor area and parietal cortices. This enhanced connectivity of motor cortex positively correlated with severity of tics measured by the Yale Global Tics Severity Scale and was not influenced by current medication status, age or gender of patients. Independently of the severity of tics, lateral and medial orbito-frontal cortex, inferior frontal, temporo-parietal junction, medial temporal and frontal pole also had enhanced structural connectivity with the striatum and thalamus in patients with Gilles de la Tourette syndrome. In addition, the cortico-striatal pathways were characterized by elevated fractional anisotropy and diminished radial diffusivity, suggesting microstructural axonal abnormalities of white matter in Gilles de la Tourette syndrome. These changes were more prominent in females with Gilles de la Tourette syndrome compared to males and were not related to the current medication status. Taken together, our data showed widespread structural abnormalities in cortico-striato-pallido-thalamic white matter pathways in patients with Gilles de la Tourette, which likely result from abnormal brain development in this syndrome.

1 Centre de Référence National Maladie Rare 'Syndrome Gilles de la Tourette', Pôle des Maladies du Système Nerveux, Groupe Hospitalier Pitié-Salpêtrière, Assistance Publique-Hôpitaux de Paris, Paris, France
2 Sorbonne Universités, UPMC Université Paris 06, UM 75, ICM, F-75013 Paris, France

3 Assistance Publique Hôpitaux de Paris (APHP), INSERM, ICM, Centre d'Investigation Clinique Pitié Neurosciences, CIC-1422, Département des Maladies du Système Nerveux, Hôpital Pitié-Salpêtrière, Paris, France
4 NeuroSpin, CEA, Gif-Sur-Yvette, France
5 Inria, Aramis project-team, Centre Paris-Rocquencourt, France
6 Centre de NeuroImagerie de Recherche – CENIR, Groupe Hospitalier Pitié-Salpêtrière, Paris, France

Correspondence to: Yulia Worbe,
Centre de Référence syndrome Gilles de la Tourette,
clinique Paul Castaigne, Hôpital Pitié-Salpêtrière,
47 – 91 boulevard de l'Hôpital, Paris,
F-75013, France.
E-mail: yworbe@gmail.com

Introduction

Gilles de la Tourette syndrome (GTS) is a childhood-onset syndrome characterized by the presence and persistence of motor and vocal tics. Convergent results from neuropathological and neuroimaging studies strongly support a dysfunction of cortico-striato-pallido-thalamo-cortical (CSPTC) networks in GTS (McNaught and Mink, 2011). Namely, neuropathological studies showed an aberrant distribution of interneurons in the caudate nucleus and putamen (Kalanithi *et al.*, 2005; Kataoka *et al.*, 2010) and both gain (Kalanithi *et al.*, 2005) and loss of projection neurons (Haber *et al.*, 1986) was reported in the globus pallidus. Corroborating these neuropathological data, numerous structural and functional neuroimaging studies also pointed to grey matter abnormalities within CSPTC pathways in GTS both in the cortex and in the basal ganglia (for review see Worbe and Hartmann, 2013).

Nonetheless, little is known about white matter organization of CSPTC pathways in GTS. Indeed, several neuroimaging studies using diffusion tensor imaging techniques pointed to structural changes in cortico-striatal pathways, the corpus callosum and the internal capsule (Thomalla *et al.*, 2009; Baumer *et al.*, 2010; Neuner *et al.*, 2010) as well as cortico-striatal pathways (Govindan *et al.*, 2010). These changes have been suggested to result both from compensatory white matter reorganization (Jackson *et al.*, 2011) and primary axonal myelinization deficits (Neuner *et al.*, 2010).

None of the studies performed to date addressed the question of structural integration among the cortex, basal ganglia structures and thalamus in GTS. In this study, we tested the hypothesis that deviant brain development in GTS would affect structural connectivity in input and output basal ganglia structures. We also address the question of white matter microstructure in patients with GTS.

Indeed, previous functional neuroimaging studies suggested delayed functional maturation of cortico-cortical and cortico-basal ganglia network both in child (Church *et al.*, 2009) and adult (Worbe *et al.*, 2012) patients with GTS. To date, the biological substrate of this putative brain maturation deficit in GTS remains unknown. In primates including humans, the typical brain development is characterized by an initial increase in neural connections, which is followed by elimination of neuronal axons (LaMantia and Rakic, 1990, 1994; Luders *et al.*, 2010). This axonal pruning during brain maturation presumably allows for a more efficient network of brain connections (Stepanyants *et al.*, 2002; Lebel *et al.*, 2008). Age-related increases in the volume of white matter during brain development likely results from increases in axonal calibre and ensheathment (Shi *et al.*, 2013; Wu *et al.*, 2013). Consequently, defects of axonal pruning as well as myelinization in GTS could lead to a less efficient function of CSPTC networks and ultimately to the development and persistence of various symptoms.

To address the aforementioned questions, we used and further implemented recently developed streamline probabilistic tractography algorithms (Marrakchi-Kacem *et al.*, 2013), which allowed us to quantify the structural integration of CSPTC networks in GTS. To further investigate the microstructure of white matter, we also evaluated fractional anisotropy and radial diffusivity ($\lambda_\perp$) in these pathways. In white matter, fractional anisotropy is sensitive to several neurobiological features, namely to the relative alignment of individual axons and their packing density (Paus, 2010). Radial diffusivity is related to histological measure of myelin density and integrity (Janve *et al.*, 2013). Taken together, these measures allowed us to evaluate white matter density and myelinization of CSPTC networks in GTS.

We primarily focused on adult patients with GTS, as we believe this population offers important insights regarding the mechanisms of symptom persistence and maintenance. Firstly, adult patients with GTS usually display a stable clinical phenotype (McGuire *et al.*, 2013). Secondly, the persistence of GTS symptoms in adulthood was suggested to result from structural alterations affecting cortico-striatal circuits and a failure of compensatory plastic changes (Peterson, 2001; Draganski *et al.*, 2010).

Materials and methods

Subjects

The local ethics committee approved the study and all participants gave written informed consent prior to the study. Sixty patients with GTS and 30 control subjects were initially included in the study. After quality check of the data based on the presence of movement artefacts, 49 patients with GTS and 28 healthy controls were finally included in the study. The groups were matched for gender (males/females: 34/15 versus 17/11; $P = 0.43$, χ-test) and age [years, mean $\pm$ standard deviation (SD): 29.89 ± 10.29 versus 29.70 ± 11.35, $P = 0.94$, two-sample t-test].

Previous to enrolment in the study, patients were recruited from the French national reference centre for GTS in Paris and examined by a multidisciplinary team. Axis I psychiatric disorders were assessed using the Mini International Neuropsychiatry Inventory by an experienced psychiatrist. The severity of tics and obsessive-compulsive disorder (OCD) symptoms was assessed using the Yale Global Tics Severity Scale (YGTSS) and Yale Brown Obsessive Compulsive scale (Y-BOCS), respectively.

For patients, inclusion criteria were aged above 18 years and confirmed DSM-IV-TR criteria for GTS. Exclusion criteria were (i) co-occurring psychopathology (current depression, substance abuse excluding tobacco, current or previous history of psychosis); and (ii) contraindications to MRI examination. Control subjects' inclusion criteria were: aged above 18 years and no history of neurological or psychiatric disorders. The exclusion criteria were the same as for patients plus previous history of tics (childhood tics) and any type of medication, excluding contraceptive pills for females.

Image acquisition

Data were acquired using a 3 T Siemens Trio TIM MRI scanner with body coil excitation and 12-channel receive phased-array head coil.

Anatomical scans were acquired using sagittal 3D T_1-weighted magnetization-prepared rapid acquisition gradient echo sequences (field of view: 256 mm; repetition time / echo time / inversion time: 2300 ms / 4.18 ms / 900 ms; flip angle: 9°; partial Fourier 7/8; one average; voxel size: $1 \times 1 \times 1$ mm^3). Diffusion weighted scans were acquired using sequences of 50 directions with a B-factor of 1000. Sixty-five slices were acquired with the following parameters: matrix 128×128, repetition time: 12 s; echo time: 87 ms; voxel size: $2 \times 2 \times 2$ mm, partial Fourier factor of 6/8, and a grappa factor of 2, read bandwidth of 1502 Hz/pixel.

Image preprocessing

T_1-weighted data

Before analysis, T_1-weighted images were visually inspected by a trained operator to detect any motion and were discarded when motion was detected, as they would prevent the definition of an accurate anatomical frame.

Whole brain masks for each subject were extracted from T_1-weighted data using BrainVISA/Morphologist (Mangin et al.,

1998). A tractography mask was computed from a whole brain mask of each subject using a previously described procedure (Guevara et al., 2011). This mask is based on anatomical information and is therefore more accurate that the classical tractography masks computed using a fractional anisotropy map threshold.

The striatum (caudate nucleus and putamen), globus pallidus (as unit including external and internal segments) and thalamus were segmented in each hemisphere of each subject using BrainVISA/Nucleist (Marrakchi-Kacem et al., 2010). Basal ganglia and thalamic volumes were measured and normalized by the total brain volume calculated from the whole brain mask. An expert (Y.W., S.o.L.), blinded to the group status of subject, checked and if necessary manually corrected the automatic segmentations.

Cortical surface and labelling of cortical gyri were obtained using Freesurfer v5.0 (Fischl et al., 1999; Desikan et al., 2006). The mesh of each subject was resampled to obtain a node-to-node correspondence between subjects (Tucholka et al., 2012). In total, 34 cortical regions in each hemisphere were included in the final analysis (Supplementary Fig. 1).

Diffusion-weighted data

The outliers due to spikes or motion were detected and corrected using a procedure previously described (Dubois et al., 2010) and implemented in BrainVISA/Connectomist-2.0 (Duclap et al., 2012).

The distortions produced by susceptibility effects due to the existence of local field inhomogeneities were estimated using the acquired B0 field map and corrected using the BrainVISA/ Connectomist 2-0 toolbox. Spikes or vibration effect and eddy currents due to the commutation of strong diffusion gradient pulses, were corrected using the Quality Check pipeline of the Connectomist toolbox used in this study (Duclap et al., 2012). Movement artefacts were detected through a comparison with the corresponding null b-value slice and corrected using an interpolation in the q-space (Dubois et al., 2010). This correction could be applied if <20 of the 50 directions were not corrupted by movements. If the movements of the subject affected >20 directions, the subject was discarded from final analysis.

Diffusion-weighted data and B0 data, as well as diffusion-weighted and T_1-weighted data were matched using a mutual information-based registration technique. The analytical Q-Ball model was applied to estimate the local underlying orientation distribution function (ODF) using a spherical harmonics order 6 and a regularization factor equal to 0.006 (Descoteaux et al., 2007). Whole brain connectivity was inferred within the previously defined domain of propagation using a streamline probabilistic tractography algorithm (Perrin et al., 2005) available in BrainVISA/Connectomist-2.0.

Connections of cortical areas with striatum and thalamus

A detailed method description of cortico-striatal and thalamo-cortical tracts selection can be found in Marrakchi-Kacem et al. (2013). Briefly, a tract was considered to intersect a nucleus (striatum or thalamus) if a minimum portion of length of the tract under consideration intersects the nucleus (typically 1.5 mm). To take into account the putative residual distortions

remaining between the diffusion-weighted data and the T_1-weighted data, a tract was considered to intersect a cortical area if its distance to its low band falls down to 2 mm (Fig. 1A). Only direct connections between striatum and cortex or thalamus were considered in the analysis: all connections going through another nucleus were discarded. The tracts were first resampled to a resolution of 0.5 mm between two consecutive points, which corresponds to half of the resolution of T_1-weighted images.

For each subject 's', nucleus 'n' and gyrus 'r', surface connectivity measures $C_s(n,r)$ were computed as previously described (Marrakchi-Kacem *et al.*, 2013). To take into account intra-subject variability, we normalized the connectivity measures by the number of whole brain tracts 'Ns' leading to normalized surface connectivity measures $NC_s(n,r)$:

$$NC_v(n, r) = C_s(n, r)/N_s$$

We previously checked that the number of whole brain tracts is not statistically different between healthy subjects and patients with GTS. We used the normalized connectivity measures in the statistical analysis.

Computation of connections of striatum with globus pallidus and thalamus

The thalamo-striatal, striato-pallidal and pallido-thalamic tracts in each subject and each hemisphere were computed using the same criteria applied for the reconstruction of cortico-striatal and thalamo-striatal connections. A tract was considered to intersect a nucleus if at least three tract points were inside this nucleus (Fig. 1B).

For every subject, for each nucleus n_1 and each nucleus n_2, normalized connectivity measures $NC(n_1,n_2)$ were computed by dividing the number of tracts linking n_1 to n_2 by the whole brain number of tracts. These normalized connectivity measures were used for the statistical analysis of the subject groups.

Computation of diffusion coefficients: fractional anisotropy and radial lambda

We further investigated scalar diffusion coefficients, i.e. fractional anisotropy and radial lambda ($\lambda_\perp$), for the connections where statistically significant group differences were found. The coefficients were measured using fractional anisotropy and $\lambda_\perp$ maps and volume connectivity maps representing in each voxel v the probability $p_C(v)$ of belonging to the tract C of interest. These probabilities were computed in each voxel by dividing the number of tracts going through the voxel by the whole brain tracts number.

For a given tract of interest, the measured scalar coefficients were obtained by averaging over the different voxels belonging to the tract the value of the scalar diffusion measure weighted by the probability of belonging to the tract. For example, for connections between the caudate nucleus and the thalamus, the measured fractional anisotropy coefficient was obtained as follows:

$$FA(caudate, thalamus) = \left(\sum_{(v \in C)} FA(v) * p_C(v)\right) / \left(\sum_{(v \in C)} p_C(v)\right),$$

where C represents the thalamo-caudate nucleus tract, FA(v) is a value of the fractional anisotropy in the voxel v and $p_C(v)$ the probability of the tract C in the voxel v.

Statistical analysis

All statistical tests were performed using SPPSS v21 statistical software (IBM inc). Before analysis, all variables were tested for Gaussian distribution (Shapiro-Wilk test, $P < 0.05$) and were transformed with square root transformation if necessary. Outlier data (>3 SD above group mean) were removed.
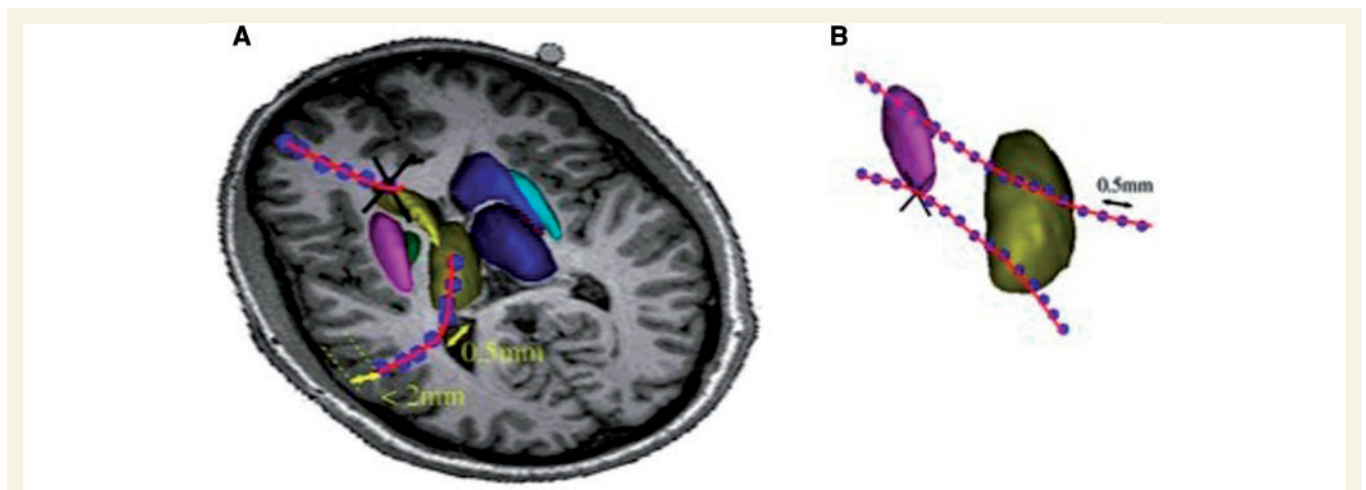

Figure 1 Selection procedure selection of neuronal tracts. (**A**) Selection of cortico-striatal and thalamo-cortical tracts. A tract was considered to intersect a nucleus (striatum or thalamus) if at least three tract points were inside the nucleus. For the cortex, only intersections with <2 mm from the low band of cortical area were considered. (**B**) Selection of tracts among basal ganglia structures and thalamus. A tract was considered for the analysis, if it intersected the nucleus at least on the three points. Black crosses represent the tracts that were rejected.

We used mixed-measures ANOVA with group (controls and patients with GTS) as independent factor and variables of interest (volumes of structures, normalized connectivity measures, fractional anisotropy, $\lambda_\perp$) as dependent factors. To access the effects related to age, gender (Hsu *et al.*, 2008) and treatment status in patients with GTS on white matter tracks, we included these variables as co-factors in a general linear model. The *post hoc* analysis was performed using Tukey's correction for multiple comparisons.

We performed a correlation analysis using partial correlation among severity of tics measured by YGTSS/50 and severity of OCD, measured by Y-BOCS/40, and values of different measures in the cortico-basal ganglia and within basal ganglia pathways with age, gender and treatment as factors of non-interest. To correct for multiple comparisons in correlation analysis, we used the FDR correction after Fisher's z-transformation of correlation coefficient r (Benjamini *et al.*, 2001).

Results

Patients with GTS

The mean severity of tics (YGTSS/50, mean ± SD) was 16.8 ± 6.8. Thirteen patients with GTS also had mild co-morbid OCD (YBOCS/40 score, mean ± SD: 12.0 ± 5.9). None of the patients with GTS had associated ADHD or other major psychiatric co-morbidities. Of the patients with GTS, 44.9% were not medicated or under behavioural therapy at the time of study; 34.7% received medication with various neuroleptics (aripiprazole, pimozide, risperidone); 12.3% were treated with selective serotonin reuptake inhibitors for co-morbid OCD and 6.1% with benzodiazepines for anxiety disorders.

Basal ganglia volumes

There was a main effect of Group [$F(1,73) = 5.390$, $P = 0.023$] and main effect of Structure (putamen, caudate nucleus, globus pallidus and thalamus) volume [$F(1,75) = 1907.884$, $P < 0.00001$] and Structure volume × Hemisphere × Group interaction [$F(1,75) = 6.935$, $P = 0.010$]. *Post hoc* analysis showed an enlargement of volumes of putamen in GTS: +4.97% on the left [$F(1,73) = 4.161$, $P = 0.045$] and +4.73% on the right [$F(1,73) = 4.078$, $P = 0.047$]. There was no statistically significant difference in volumes of other basal ganglia structures or thalamus. There were no effects of age, gender or treatment (all $P > 0.50$) on basal ganglia volumes or correlations with YGTSS and Y-BOCS scores (all $P > 0.40$).

Cortico-striatal and thalamo-striatal connections in GTS

There was a main effect of Group [$F(1,221) = 3.922$, $P = 0.049$] and Region × Group interaction [$F(1,221) = 5.466$,

$P = 0.020$]. *Post hoc* analysis showed that 14 of 34 cortical regions in GTS had abnormally enhanced structural connectivity between the striatum and thalamus in the left hemisphere (LH) [main effect of group: $F(1,227) = 2.989$, $P = 0.001$] and seven regions in the right hemisphere (RH) [main effect of group: $F(1,227) = 2.065$, $P = 0.002$]. Fusiform gyrus, anterior and middle cingulate cortex had diminished connections with the striatum and thalamus in the left hemisphere (Table 1 and Fig. 2A–C).

There was no effect of age in both groups (both $P > 0.10$). We found the effect of gender in GTS [$F(1,145) = 7.599$; $P = 0.007$] and GTS × Gender interaction [$F(1,145) = 4.594$, $P = 0.034$] but not effect of gender in controls [$F(1,81) = 0.275$; $P = 0.601$].

On *post hoc* analysis, in GTS females compared to males, there were more connections between the striatum, thalamus and the cortical areas as follows: temporal junction [LH: $F(1,45) = 19.678$, RH: $F(1,45) = 10.674$, both $P < 0.0001$], inferior [LH: $F(1,45) = 21.864$, RH: $F(1,45) = 17.585$, both $P < 0.0001$] and superior parietal cortices [LH: $F(1,45) = 14.907$, $P < 0.0001$], lateral orbito-frontal cortex [LH: $F(1,45) = 5.717$, $P = 0.018$; RH: $F(1,45) = 9.083$, $P = 0.003$], middle temporal cortex [LH: $F(1,45) = 20.740$, $P < 0.0001$; RH: $F(1,45) = 10.285$, $P = 0.002$], primary sensory [LH: $F(1,45) = 12.175$, $P = 0.001$] and motor cortices [LH: $F(1,45) = 13.163$, $P < 0.0001$]. There was no effect of treatment on cortico-striatal and cortico-thalamic connections in GTS [$F(1,143) = 0.165$, $P = 0.685$].

Connexions among basal ganglia structures and thalamus in GTS

Striato-pallidal, including putamino-pallidal and caudo-pallidal pathways, as well as thalamo-striatal (thalamo-putaminal and thalamo-caudal) and pallido-thalamic pathways in both hemispheres were included in the statistical analysis. There was a main effect of Group [$F(1,75) = 26.854$, $P < 0.001$], main effect of Pathway [$F(1,75) = 1000.116$, $P < 0.0001$] and Group × Pathway × Hemisphere interaction [$F(1,75) = 5.493$, $P = 0.021$].

In *post hoc* analysis, in patients with GTS there was an elevated proportion of structural connections between the thalamus and the putamen bilaterally [LH: $F(1,75) = 4.153$, $P = 0.045$; RH: $F(1,75) = 5.875$, $P = 0.018$] and a trend to more structural connections between putamen and globus pallidus on the left [$F(1,75) = 4.140$, $P = 0.063$] (Fig. 3).

There was no effect of gender on thalamo-putaminal connections in any group (both $P > 0.17$). There was an effect of age in controls [$F(1,25) = 5.249$, $P = 0.031$] but not in patients with GTS [$F(1,45) = 1.560$, $P = 0.218$]. There was no effect of treatment [$F(1,45) = 0.221$, $P = 0.641$] in patients with GTS.

Table 1 Abnormal structural connectivity of cortico-striatal and thalamo-cortical pathways in patients with GTS

Cortical area	Side	Connectivity	F	P	FA	F	P	$\lambda\perp$	F	P
Temporo-parietal junction	L	↑	8.228	<0.0001	↑	6.189	0.014			
	R	↑	3.984	0.009						
Anterior cingulate cortex	L	↓	5.664	0.001	↑	4.151	0.043	↓	6.682	0.010
Fusiform gurus	L	↓	3.047	0.030	↑	10.695	0.001	↓	7.777	0.006
	R				↑	8.300	0.004			
Inferior parietal cortex	L	↑	9.589	<0.0001						
	R	↑	7.513	<0.0001	↑	6.029	0.015			
Lateral orbito-frontal cortex	L	↑	3.583	0.015				↓	7.416	0.007
	R	↑	2.788	0.041						
Medial orbito-frontal cortex	L	↑	3.379	0.019	↑	7.915	0.005	↓	16.001	<0.0001
Middle temporal cortex	L	↑	6.123	0.001	↑	8.473	0.004			
	R	↑	3.724	0.012						
Paracentral lobule and SMA	L	↑	2.948	0.034	↑	9.792	0.002			
Inferior frontal gurus	L	↑	6.395	<0.0001						
	R	↑	5.983	0.001						
Primary sensory cortex	L	↑	6.874	<0.0001				↓	5.277	0.023
	R	↑	6.289	<0.0001						
Middle cingulate cortex	L	↓	2.803	0.041				↓	3.929	0.049
Primary motor cortex	L	↑	3.612	0.014	↑	5.668	0.018	↓	10.366	< 0.0001
Frontal pole	L	↑	3.781	0.011						
	R	↑	5.756	0.001						
Superior parietal cortex	L	↑	4.948	0.002						
	R	↑	9.346	<0.0001						

L = left hemisphere, R = right hemisphere; ↑ = enhanced structural connectivity in GTS compared to healthy controls; ↓ = diminished structural connectivity in GTS compared to healthy controls; FA = fractional anisotropy; $\lambda_\perp$ = radial diffusivity coefficient; SMA = supplementary motor cortex.
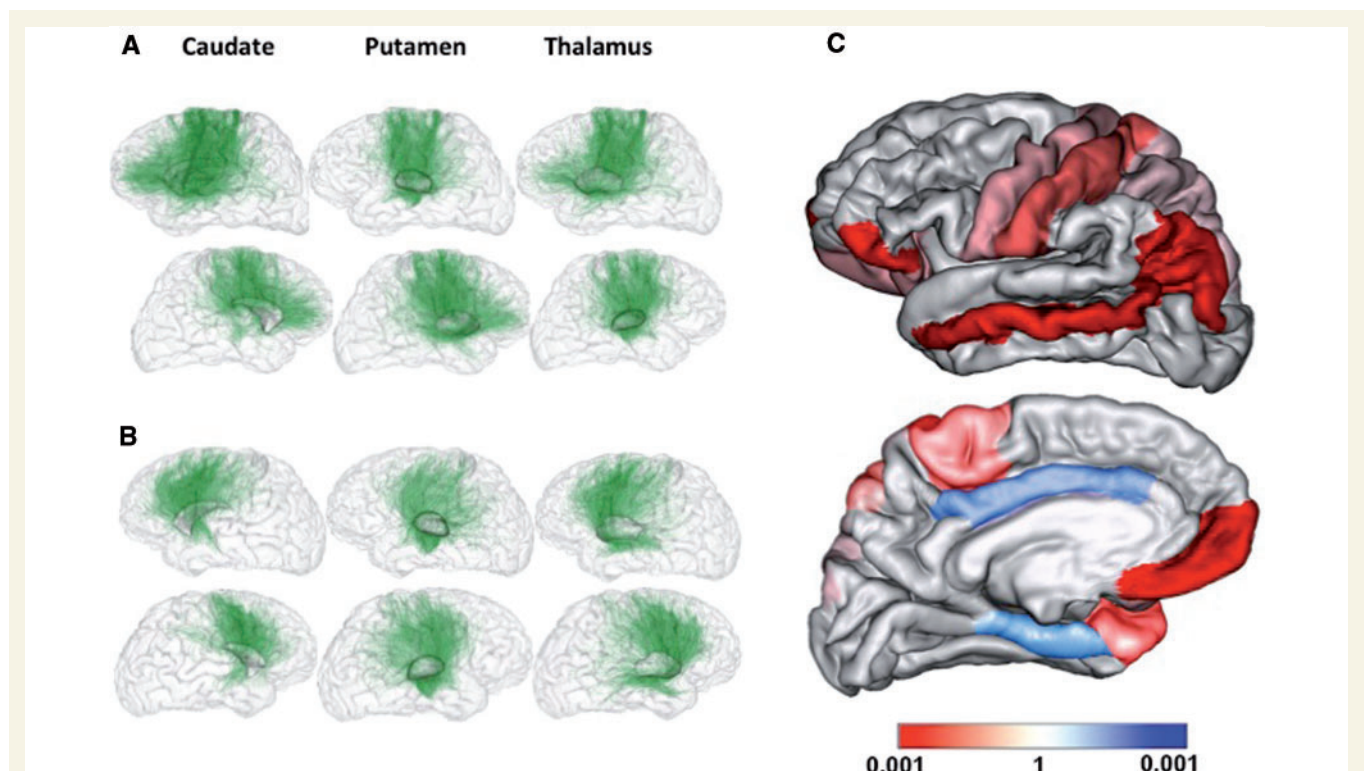

Figure 2 Cortico-striatal and thalamo-striatal tracts. (A and B) Individual level: (**A**) GTS patient, (**B**) healthy control. The *top row* represents the right hemisphere and the *bottom row* the left hemisphere. (**C**) Differences on group level analysis: in red are the cortical areas with enhanced structural connectivity in patients with GTS compared to controls; in blue are the cortical areas with diminished structural connectivity in patients with GTS compared to controls. The differences in structural connectivity of both hemispheres are projected to the cortical areas of the left hemisphere.
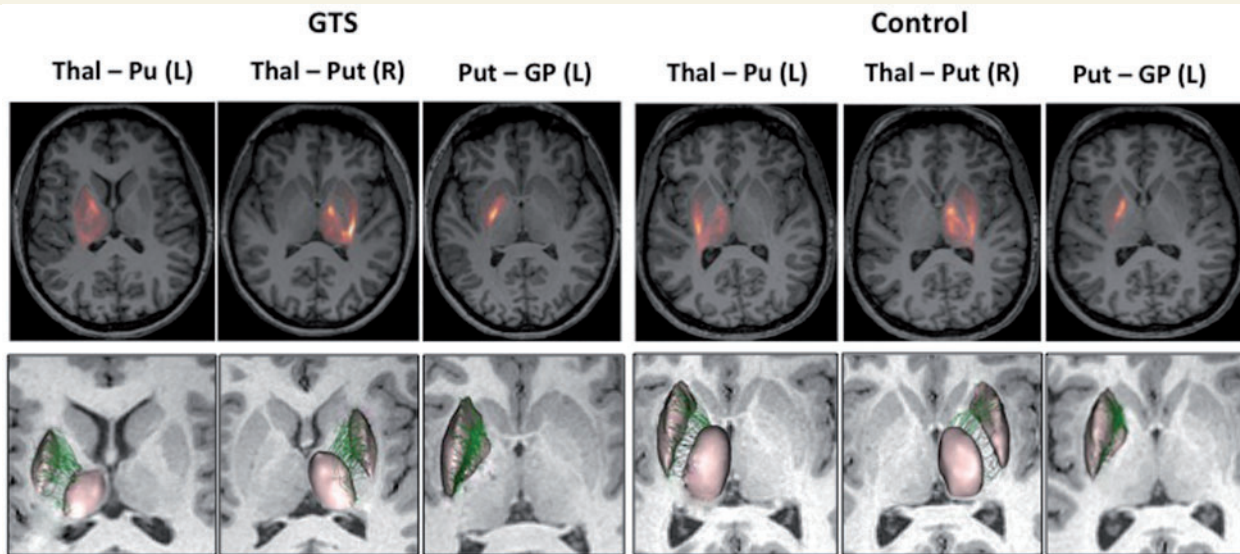
Figure 3 Individual thalamo-strital and striato-pallidal connections in patients with GTS and controls. *Top row*: The density of connections map on individual level; *Bottom row*: Thalamo-striatal and striato-pallidal connections on individual level. Only connections with statistically significant difference in structural connectivity on group level are illustrated. L = left; R = right; Thal-Pu(t) = thalamo-putaminal connections; Put-GP = putamen-globus pallidus connections.

Measures of fractional anisotropy and radial lambda in the CSPTC network

To further evaluate the microstructural integrity of white matter pathways, we also computed the fractional anisotropy and the radial lambda ($\lambda_\perp$) in the cortico-striatal, thalamo-cortical, striato-pallidal, thalamo-striatal and pallido-thalamic pathways.

For cortico-striatal and thalamo-cortical pathways, there was a main effect of GTS diagnosis [fractional anisotropy: $F(1,227) = 6.000$, $P < 0.001$; $\lambda_\perp$: $F(1,227) = 5.445$, $P < 0.001$], where in *post hoc* comparisons, patients with GTS had elevated fractional anisotropy and diminished values of $\lambda_\perp$ in the tracts connecting the cortex with the striatum and thalamus (Table 1).

There was no effect of gender (both groups, $P > 0.05$) but there was an effect of age [healthy controls: $F(1,81) = 5.52$, $P = 0.020$; GTS: $F(1,144) = 12.300$, $P < 0.001$] on the fractional anisotropy. In GTS, there was an effect of gender [$F(1,144) = 15.757$, $P < 0.001$] and age [$F(1,144) = 6.389$, $P = 0.013$] on $\lambda_\perp$, which was absent in healthy controls (both $P > 0.1$). There was no effect of treatment on fractional anisotropy [$F(1,45) = 0.002$, $P = 0.963$] or on $\lambda_\perp$ [$F(1,45) = 0.019$, $P = 0.889$] in cortico-striatal and cortico-thalamic tracts in GTS.

In basal ganglia pathways, we found elevated fractional anisotropy in the left thalamo-putaminal tract [$F(1,74) = 5.325$, $P = 0.022$], diminished $\lambda_\perp$ in the left thalamo-putaminal tract [$F(1,74) = 6.43$, $P = 0.013$] and a trend for elevated $\lambda_\perp$ in the left pallido-thalamic tract [$F(1,73) = 3.091$, $P = 0.061$] in patients with GTS compared

to healthy controls. There were no differences based on age or gender in both groups on these pathways. In patients with GTS, there was no effect of treatment on these pathways.

Correlations of structural changes in CSPTC networks with severity of tics and OCD

The severity of tics measured by the YGTSS/50 positively correlated with cortico-striatal, thalamo-cortical pathways and with the structural connectivity between the putamen and the thalamus as listed in Table 2. We did not find any statistically significant correlations between YGTSS subscores and structural connectivity values in cortico-striatal and thalamo-cortical pathways (all $P > 0.05$).

OCD symptom severity measured by the Y-BOCS was positively correlated with structural connectivity of the striatum with the orbito-frontal cortex and the left thalamo-putaminal tract (Table 2).

Discussion

In patients with GTS, we showed white matter abnormalities in pathways connecting cerebral cortex, basal ganglia and thalamus. Namely, a greater volume of putamen was associated with greater numbers of connections with cortical areas, thalamus and globus pallidus. Moreover, the cortico-striatal pathways were also characterized by elevated fractional anisotropy and diminished radial

Table 2 Correlations of structural changes with severity of tics and OCD symptoms in patients with GTS

Region	Hemisphere	r	Z-score	P-value
Yale Global Tics Severity Scale (YGTSS/50):				
Cortico-striatal and thalamo-cortical pathways:				
Inferior frontal gyrus	L	0.189	2.25	0.012
	R	0.175	2.08	0.018
Primary motor cortex	L	0.169	2.01	0.022
	R	0.167	1.98	0.023
Supplementary motor area (ventral part)	L	0.168	1.99	0.023
Cingulate cortex (middle part)	L	−0.170	2.02	0.021
Within basal ganglia structures:				
Thalamo-putaminal tract	L	0.270	3.26	<0.005
	R	0.378	4.09	<0.0001
Yale Brown Obsessive Compulsive scale (Y-BOCS/40):				
Cortico-striatal and thalamo-cortical pathways:				
Orbito-frontal cortex (anterior part)	R	0.204	2.43	0.007
Orbito-frontal cortex (medial part)	R	0.221	2.64	0.004
Within basal ganglia structures:				
Thalamo-putaminal tract	L	0.304	3.70	< 0.0001

L = left hemisphere; R = right hemisphere.

diffusivity, suggesting microstructural axonal abnormalities of white matter tracts in patients with GTS. Our data also showed a possible gender dimorphism in GTS as these changes were more prominent in females with GTS compared to males and were not related to the current medication status.

Abnormal cortical connections with striatum and thalamus in GTS

A novel diffusion tensor imaging approach used in this study allowed us to project the connectivity of each basal ganglia structure directly onto the cortical surface. We were able to determine a selective region-specific alteration of cortical connections with the striatum and thalamus and to quantify connectivity differences between basal ganglia structures and cortical areas.

Indeed, previous studies using probabilistic diffusion tractography and tract-based spatial statistics methods have already pointed to widespread white matter abnormalities in adult patients with GTS, including corpus callosum, anterior capsula, inferior fronto-occipital fasciculus, the superior longitudinal fasciculus and fasculus uncinatus (Neuner et al., 2010) and cortico-striatal networks (Govindan et al., 2010). Convergent with these results, our data also showed that several cortical regions had abnormal structural connectivity with the striatum and the thalamus in GTS. Specifically, in the motor pathway, primary motor and sensory cortices, as well as paracentral lobule, supplementary motor area and parietal cortices had abnormally enhanced structural connectivity with the striatum and thalamus. The enhanced connectivity of motor cortex and supplementary motor area positively correlated with tic severity and was

independent of the current medication status, age or gender of the patients with GTS. These results corroborate numerous structural and functional neuroimaging studies (for reviews see Plessen et al., 2009; Felling and Singer, 2011), which suggested primary grey matter abnormalities in motor pathway related to tics. Nonetheless, previous studies using deterministic diffusion tensor imaging methods showed discrepant results with both enhanced (Thomalla et al., 2009) and no difference (Thomalla et al., 2013) in white matter underlying sensorimotor cortex. Another study on adult patients with GTS showed reduction of structural connectivity of the supplementary motor cortex with the striatum, which also negatively predicted severity of tics (Cheng et al., 2014). The discrepancy with our data could result from methodological differences (data preprocessing, artefacts correction and diffusion tensor imaging models applied) and small groups ($n = 15$) of patients with GTS included in these studies.

Beyond motor pathways, several cortical areas, namely lateral and medial orbito-frontal, inferior frontal, as well as temporo-parietal junction, medial temporal and frontal pole had enhanced structural connections with the striatum and thalamus in GTS independently of the severity of tics (i.e. no correlation with the YGTSS). Structural abnormalities in frontal, parietal and cingulate cortex have been previously described in GTS (Muller-Vahl et al., 2009; Wittfoth et al., 2012) and could be potentially related to expression of complex tics (Worbe et al., 2010). Nonetheless, we did not find a correlation of complexity subscores of the YGTSS with structural changes in these white matter pathways. Alternatively, taking into account that these cortical areas are largely involved in behavioural stopping and switching (Aron et al., 2004; Swann et al., 2009; Philipp et al., 2012) and that patients with GTS

often display an enhanced cognitive control over their movements (Mueller *et al.*, 2006), white matter structural changes could also reflect plastic brain reorganization in GTS, as was suggested by previous studies (Jackson *et al.*, 2011).

Finally, some of these structural changes could be related to the presence of co-morbidities. Indeed, the severity of OCD in adult patients with GTS was positively correlated to structural connections of the striatum and thalamus with the medial orbito-frontal cortex, which is in line with previous studies showing orbito-frontal cortex involvement in OCD without tics (Radua *et al.*, 2010; Meunier *et al.*, 2012).

Interestingly, we found a sexual dimorphism in cortico-striatal and thalamo-cortical pathways with more structural connections in females with GTS compared to males. Previous studies pointed to sexual dimorphism in the clinical presentation in GTS (Lewin *et al.*, 2012; Rodgers *et al.*, 2013). Gender differences were also evidenced on cortical and basal ganglia structure levels in structural neuroimaging studies in children with GTS and to a less extent in adults with GTS (Zimmerman *et al.*, 2000; Peterson *et al.*, 2001; Fahim *et al.*, 2010). Our data extend these findings to white matter and cortico-striatal and thalamo-cortical pathways.

Microstructural changes of cortico-striatal white matter pathways in GTS

Another characteristic of cortico-striatal pathways in GTS was increased values of fractional anisotropy and decreased values of radial diffusivity. These diffusion coefficients are suggested to reflect the microstructural organization of white matter. In particular, studies of histological-radiological correlations in animal models pointed to the strong relationship of radial diffusivity with myelin density, where the lack of myelin is indexed by increase of radial diffusivity (Song *et al.*, 2002; Janve *et al.*, 2013). In contrast, fractional anisotropy was shown to be more related to axonal package density and less to myelin ensheathment (Winston, 2012). So far, our data could suggest a higher axonal density and dysmyelination (with potential enlargement of myelin sheets) of cortico-striatal pathways in patients with GTS. Alternatively, a lower angular dispersion of axon directionality as well as alterations of the extra-axonal space in GTS patients could also be considered. More complex diffusion microstructural models such as CHARMED (Composite Hindered and Restricted Model of Diffusion) or AxCaliber (Assaf *et al.*, 2008) could indeed address the question of axonal diameters in patients with GTS with greater precision; nonetheless the clinical application of these models is restricted by a long duration of data acquisition, which is difficult for patients with tics. A recently developed Myelin Water Fraction mapping

technique could also be used in further studies to better quantify myelin ensheathment (Deoni *et al.*, 2012).

Abnormal thalamo-striatal connections in GTS

In basal ganglia pathways, we found enhanced structural connectivity in thalamo-putaminal pathways bilaterally. In addition, we found a strong positive correlation of structural changes in thalamo-putaminal tracts with severity of tics. As a large part of the putamen is involved in the processing of motor information (Parent and Parent, 2006), the present data support the involvement of motor network in the genesis of tics. To date, the exact information flow along thalamo-striatal pathways and its functional relevance for basal ganglia function remains largely unknown. Several studies suggested that thalamo-striatal projections might play the role of positive reinforcer for striatal neurons involved in performing a selected behaviour (Smith *et al.*, 2004) or in monitoring of 'top-down' control through modulation of activity of cortico-basal ganglia loops (Kimura *et al.*, 2004).

These white matter structural changes were also associated with larger volumes of putamen in both hemispheres. Enlargement of putaminal volume has already been reported in children (Ludolph *et al.*, 2006) but not in adults with GTS. Nonetheless, previous studies on a large group of patients with GTS with an extensive age range (Peterson *et al.*, 2003) showed that age-related reduction of basal ganglia volumes was smaller in adult patients with GTS compared to controls. Accordingly, our findings could potentially reflect the slower reduction in putaminal volume in GTS compared to age-matched controls, which support the slower brain maturation hypothesis of GTS. Nonetheless, we cannot completely exclude that enlargement of putaminal volumes results from exposure to neuroleptics, even over a short period of time, as was suggested by previous studies (Peterson *et al.*, 2003).

Conclusion

Using a novel diffusion tensor imaging method and large patient group, we showed structural abnormalities in cortico-striato-pallido-thalamic white matter pathways in patients with GTS compared to healthy controls. These structural abnormalities could arise from a higher density and myelin ensheathment of neuronal axons and potentially result from abnormal trajectory of brain maturation in GTS and a failure of plastic compensatory brain mechanisms. Further DTI studies with advanced models will be required to answer these questions. Also, it is worth mentioning that these results reflect structural changes in adult patients with GTS, which likely would differ from those that could be observed in children with GTS (Plessen *et al.*, 2009).

Acknowledgements

Funding

Supplementary material

Supplementary material is available at *Brain* online.

References

Aron AR, Monsell S, Sahakian BJ, Robbins TW. A componential analysis of task-switching deficits associated with lesions of left and right frontal cortex. Brain 2004; 127: 1561–73.

Assaf Y, Blumenfeld-Katzir T, Yovel Y, Basser PJ. AxCaliber: a method for measuring axon diameter distribution from diffusion MRI. Magn Reson Med 2008; 59: 1347–54.

Baumer T, Thomalla G, Kroeger J, Jonas M, Gerloff C, Hummel FC, et al. Interhemispheric motor networks are abnormal in patients with Gilles de la Tourette syndrome. Mov Disord 2010; 25: 2828–37.

Benjamini Y, Drai D, Elmer G, Kafkafi N, Golani I. Controlling the false discovery rate in behavior genetics research. Behav Brain Res 2001; 125: 279–84.

Cheng B, Braass H, Ganos C, Treszl A, Biermann-Ruben K, Hummel FC, et al. Altered intrahemispheric structural connectivity in Gilles de la Tourette syndrome. Neuroimage Clin 2014; 7: 174–81.

Church JA, Fair DA, Dosenbach NU, Cohen AL, Miezin FM, Petersen SE, et al. Control networks in paediatric Tourette syndrome show immature and anomalous patterns of functional connectivity. Brain 2009; 132: 225–38.

Deoni SC, Dean DCD, O'Muircheartaigh J, Dirks H, Jerskey BA. Investigating white matter development in infancy and and early childhood using myelin water faction and relaxation time mapping. Neuroimage 2012; 63: 1038–53.

Descoteaux M, Angelino E, Fitzgibbons S, Deriche R. Regularized, fast, and robust analytical Q-ball imaging. Magn Reson Med 2007; 58: 497–510.

Desikan RS, Segonne F, Fischl B, Quinn BT, Dickerson BC, Blacker D, et al. An automated labeling system for subdividing the human cerebral cortex on MRI scans into gyral based regions of interest. Neuroimage 2006; 31: 968–80.

Draganski B, Martino D, Cavanna AE, Hutton C, Orth M, Robertson MM, et al. Multispectral brain morphometry in Tourette syndrome persisting into adulthood. Brain 2010; 133: 3661–75.

Dubois J, Dehaene-Lambertz G, Hertz-Pannier L, Santoro G, Mangin J-F, Poupon C. Correction strategy for infants diffusion-weighted images corrupted with motion. Proceedings of the ISMRM 17th Annual Meeting, Stockholm, Sweden. 2010.

Duclap D, Schmitt B, Lebois A, Riff O, Guevara P, Marrakchi-Kacem L, et al. Connectomist-2.0: a novel diffusion analysis toolbox for BrainVISA. European Society for Magnetic Resonance in Medicine and Biology. Lisbon, Portugal: Springer; 2012.

Fahim C, Yoon U, Das S, Lyttleton O, Chen J, Arnaoutelis R, et al. Somatosensory-motor bodily representation cortical thinning in Tourette: effects of tic severity, age and gender. Cortex 2010; 46: 750–60.

Felling RJ, Singer HS. Neurobiology of tourette syndrome: current status and need for further investigation. J Neurosci 2011; 31: 12387–95.

Fischl B, Sereno MI, Tootell RB, Dale AM. High-resolution intersubject averaging and a coordinate system for the cortical surface. Hum Brain Mapp 1999; 8: 272–84.

Govindan RM, Makki MI, Wilson BJ, Behen ME, Chugani HT. Abnormal water diffusuvity in cortico-striatal projections in children with Tourette syndrome. Hum Brain Mapp 2010; 31: 1665–74.

Guevara P, Poupon C, Riviere D, Cointepas Y, Descoteaux M, Thirion B, et al. Robust clustering of massive tractography datasets. Neuroimage 2011; 54: 1975–93.

Haber SN, Kowall NW, Vonsattel JP, Bird ED, Richardson EP Jr. Gilles de la Tourette's syndrome. A postmortem neuropathological and immunohistochemical study. J Neurol Sci 1986; 75: 225–41.

Hsu JL, Leemans A, Bai CH, Lee CH, Tsai YF, Chiu HC, et al. Gender differences and age-related white matter changes of the human brain: a diffusion tensor imaging study. Neuroimage 2008; 39: 566–77.

Jackson SR, Parkinson A, Jung J, Ryan SE, Morgan PS, Hollis C, et al. Compensatory neural reorganization in Tourette syndrome. Curr Biol 2011; 21: 580–585.

Janve VA, Zu Z, Yao SY, Li K, Zhang FL, Wilson KJ, et al. The radial diffusivity and magnetization transfer pool size ratio are sensitive markers for demyelination in a rat model of type III multiple sclerosis (MS) lesions. Neuroimage 2013; 74: 298–305.

Kalanithi PS, Zheng W, Kataoka Y, DiFiglia M, Grantz H, Saper CB, et al. Altered parvalbumin-positive neuron distribution in basal ganglia of individuals with Tourette syndrome. Proc Natl Acad Sci USA 2005; 102: 13307–12.

Kataoka Y, Kalanithi PS, Grantz H, Schwartz ML, Saper C, Leckman JF, et al. Decreased number of parvalbumin and cholinergic interneurons in the striatum of individuals with Tourette syndrome. J Comp Neurol 2010; 518: 277–91.

Kimura M, Minamimoto T, Matsumoto N, Hori Y. Monitoring and switching of cortico-basal ganglia loop functions by the thalamo-striatal system. Neurosci Res 2004; 48: 355–60.

LaMantia AS, Rakic P. Axon overproduction and elimination in the corpus callosum of the developing rhesus monkey. J Neurosci 1990; 10: 2156–75.

LaMantia AS, Rakic P. Axon overproduction and elimination in the anterior commissure of the developing rhesus monkey. J Comp Neurol 1994; 340: 328–36.

Lebel C, Walker L, Leemans A, Phillips L, Beaulieu C. Microstructural maturation of the human brain from childhood to adulthood. Neuroimage 2008; 40: 1044–55.

Lewin AB, Murphy TK, Storch EA, Conelea CA, Woods DW, Scahill LD, et al. A phenomenological investigation of women with Tourette or other chronic tic disorders. Compr Psychiatry 2012; 53: 525–34.

Luders E, Thompson PM, Toga AW. The development of the corpus callosum in the healthy human brain. J Neurosci 2010; 30: 10985–90.

Ludolph AG, Juengling FD, Libal G, Ludolph AC, Fegert JM, Kassubek J. Grey-matter abnormalities in boys with Tourette syndrome: magnetic resonance imaging study using optimised voxel-based morphometry. Br J Psychiatry 2006; 188: 484–5.

Mangin JF, Coulon O, Frouin V. Robust brain segmentation using histogram scale-space analysis and mathematical morphology'. In: Wells WM, Colchester A, Delp S, editors. Proc 1st MICCAI, LNCS-1496. Boston: MIT; 1998. p. 1230–41.

Marrakchi-Kacem L, Delmaire C, Guevara P, Poupon F, Lecomte S, Tucholka A, et al. Mapping cortico-striatal connectivity onto the cortical surface: a new tractography-based approach to study Huntington disease. PLoS One 2013; 8: e53135.

Marrakchi-Kacem L, Poupon C, Mangin JF, Poupon F. Multi-contrast deep nuclei segmentation using a probabilistic atlas. Proceedings of the IEEE International Symposium on Biomedical Imaging. 2010. p. 61–4.

McGuire JF, Nyirabahizi E, Kircanski K, Piacentini J, Peterson AL, Woods DW, et al. A cluster analysis of tic symptoms in children and adults with Tourette syndrome: clinical correlates and treatment outcome. Psychiatry Res 2013; 210: 1198–204.

McNaught KS, Mink JW. Advances in understanding and treatment of Tourette syndrome. Nat Rev Neurol 2011; 7: 667–76.

Meunier D, Ersche KD, Craig KJ, Fornito A, Merlo-Pich E, Fineberg NA, et al. Brain functional connectivity in stimulant drug dependence and obsessive-compulsive disorder. Neuroimage 2012; 59: 1461–8.

Mueller SC, Jackson GM, Dhalla R, Datsopoulos S, Hollis CP. Enhanced cognitive control in young people with Tourette's syndrome. Curr Biol 2006; 16: 570–3.

Muller-Vahl KR, Kaufmann J, Grosskreutz J, Dengler R, Emrich HM, Peschel T. Prefrontal and anterior cingulate cortex abnormalities in Tourette Syndrome: evidence from voxel-based morphometry and magnetization transfer imaging. BMC Neurosci 2009; 10: 47.

Neuner I, Kupriyanova Y, Stocker T, Huang R, Posnansky O, Schneider F, et al. White-matter abnormalities in Tourette syndrome extend beyond motor pathways. Neuroimage 2010; 51: 1184–93.

Parent M, Parent A. Single-axon tracing study of corticostriatal projections arising from primary motor cortex in primates. J Comp Neurol 2006; 496: 202–13.

Paus T. Growth of white matter in the adolescent brain: myelin or axon? Brain Cogn 2010; 72: 26–35.

Perrin M, Poupon C, Cointepas Y, Rieul B, Golestani N, Pallier C, et al. Fiber tracking in q-ball fields using regularized particle trajectories. In: Proceedings IPMI, Glenwood Springs, Colorado, 2005.

Peterson BS. Neuroimaging studies of Tourette syndrome: a decade of progress. Adv Neurol 2001; 85: 179–96.

Peterson BS, Staib L, Scahill L, Zhang H, Anderson C, Leckman JF, et al. Regional brain and ventricular volumes in Tourette syndrome. Arch Gen Psychiatry 2001; 58: 427–40.

Peterson BS, Thomas P, Kane MJ, Scahill L, Zhang H, Bronen R, et al. Basal Ganglia volumes in patients with Gilles de la Tourette syndrome. Arch Gen Psychiatry 2003; 60: 415–24.

Philipp AM, Weidner R, Koch I, Fink GR. Differential roles of inferior frontal and inferior parietal cortex in task switching: evidence from stimulus-categorization switching and response-modality switching. Hum Brain Mapp 2012; 34: 1910–20.

Plessen KJ, Bansal R, Peterson BS. Imaging evidence for anatomical disturbances and neuroplastic compensation in persons with Tourette syndrome. J Psychosom Res 2009; 67: 559–73.

Radua J, van den Heuvel OA, Surguladze S, Mataix-Cols D. Meta-analytical comparison of voxel-based morphometry studies in obsessive-compulsive disorder vs other anxiety disorders. Arch Gen Psychiatry 2010; 67: 701–11.

Rodgers S, Muller M, Kawohl W, Knopfli D, Rossler W, Castelao E, et al. Sex-related and non-sex-related comorbidity subtypes of tic disorders: a latent class approach. Eur J Neurol 2013; 21: 700–7.

Shi Y, Short SJ, Kinickmeyer RC, Wang J, Coe CL, Neithammer M, et al. Diffusuin tensor imaging-based characterization of brain neurodevelopment in primates. Cerebral Cortex 2013; 23: 36–48.

Smith Y, Raju DV, Pare JF, Sidibe M. The thalamostriatal system: a highly specific network of the basal ganglia circuitry. Trends Neurosci 2004; 27: 520–7.

Song SK, Sun SW, Rambsbottom MJ, Chang C, Russel J, Cross AH. Dysmielination revealed through MRI as increased radial (but unchanged axial) diffusion of water. Neuroimage 2002; 17: 1429–36.

Stepanyants A, Hof PR, Chklovskii DB. Geometry and structural plasticity of synaptic connectivity. Neuron 2002; 34: 275–88.

Swann N, Tandon N, Canolty R, Ellmore TM, McEvoy LK, Dreyer S, et al. Intracranial EEG reveals a time- and frequency-specific role for the right inferior frontal gyrus and primary motor cortex in stopping initiated responses. J Neurosci 2009; 29: 12675–85.

Thomalla G, Jonas M, Baumer T, Siebner HR, Biermann-Ruben K, Ganos C, et al. Cost of control: descreased motor cortex engagement during a Go/No Go task in Tourette's syndrome. Brain 2013; 137: 122–36.

Thomalla G, Siebner HR, Jonas M, Baumer T, Biermann-Ruben K, Hummel F, et al. Structural changes in the somatosensory system correlate with tic severity in Gilles de la Tourette syndrome. Brain 2009; 132: 765–77.

Tucholka A, Fritsch V, Poline JB, Thirion B. An empirical comparison of surface-based and volume-based group studies in neuroimaging. Neuroimage 2012; 63: 1443–53.

Winston GP. The physical and biological basis of quantitative parameters from diffusion MRI. Quant Imaging Med Surg 2012; 2: 254–65.

Wittfoth M, Bornmann S, Peschel T, Grosskreutz J, Glahn A, Buddensiek N, et al. Lateral frontal cortex volume reduction in Tourette syndrome revealed by VBM. BMC Neurosci 2012; 13: 17.

Worbe Y, Gerardin E, Hartmann A, Valabregue R, Chupin M, Tremblay L, et al. Distinct structural changes underpin clinical phenotypes in patients with Gilles de la Tourette syndrome. Brain 2010; 133: 3649–60.

Worbe Y, Hartmann A. Neuroimaging of Gilles de la Tourette syndrome. In: Tuite P, Dagher A, editors. Magenetic resonance imaging in movement disorders. Cambridge University Press; 2013. p. 121–34.

Worbe Y, Malherbe C, Hartmann A, Pelegrini-Issac M, Messe A, Vidailhet M, et al. Functional immaturity of cortico-basal ganglia networks in Gilles de la Tourette syndrome. Brain 2012; 135: 1937–46.

Wu M, Lu LH, Lowes A, Yang S, Passarotti AM, Zhou XJ, et al. Development of surfacial white matter and its structural interplay with cortical grey matter in children and adolescents. Hum Brain Mapp 2013; 35: 2806–16.

Zimmerman AM, Abrams MT, Giuliano JD, Denckla MB, Singer HS. Subcortical volumes in girls with tourette syndrome: support for a gender effect. Neurology 2000; 54: 2224–9.